

Fast-timing measurements in neutron-rich odd-mass zirconium isotopes using LaBr₃:Ce detectors coupled with Gammasphere

E. R. Gamba^{1,*}, S. Lalkovski^{2,3}, M. Rudigier², A. M. Bruce¹, S. Bottoni⁴, M. P. Carpenter⁴, S. Zhu⁴, A. D. Ayangeakaa⁴, J. T. Anderson⁴, T. A. Berry², I. Burrows⁵, R. J. Carroll², P. Copp⁶, M. Carmona Gallardo⁷, D. M. Cullen⁸, T. Daniel², J. P. Greene⁴, L. A. Gurgi², D. J. Hartley⁹, R. Ilieva², S. Ilieva¹⁰, R. V. F. Janssens³, F. G. Kondev¹¹, T. Kröll¹⁰, G. J. Lane¹², T. Lauritsen⁴, I. Lazarus⁵, G. Lotay², G. Fernández Martínez¹⁰, Zs. Podolyák², V. Pucknell⁵, M. Reed¹², P. H. Regan^{2,13}, J. Rohrer⁴, J. Sethi⁴, D. Seweryniak⁴, C. M. Shand², J. Simpson⁵, M. Smolen¹⁴, E. A. Stefanova¹⁵, V. Vedia⁷, and O. Yordanov¹⁵

¹School of Computing, Engineering and Mathematics, University of Brighton, Brighton BN2 4JG, UK

²Department of Physics, University of Surrey, Guildford GU2 7XH, UK

³Department of Nuclear Engineering, Faculty of Physics, University of Sofia "St. Kl. Ohridski", Sofia 1164, Bulgaria

⁴Physics Division, Argonne National Laboratory, Argonne, Illinois 60439, USA

⁵STFC Daresbury Laboratory, Daresbury, Warrington WA4 4AD, UK

⁶Department of Physics and Applied Physics, University of Massachusetts Lowell, Lowell, Massachusetts 01854, USA

⁷Grupo de Física Nuclear, Universidad Complutense, CEI Moncloa, ES-28040 Madrid, Spain

⁸School of Physics and Astronomy, University of Manchester, Manchester M13 9PL, UK

⁹Department of Physics, U.S. Naval Academy, Annapolis, Maryland 21402, USA

¹⁰Institut für Kernphysik, TU Darmstadt, Schlossgartenstrasse 9, 64289 Darmstadt, Germany

¹¹Nuclear Engineering Division, Argonne National Laboratory, Argonne, Illinois 60439, USA

¹²Department of Nuclear Physics, R.S.P.E., Australian National University, Canberra 0200, Australia

¹³AIR Division, NPL, Teddington, TW11 0LW, UK

¹⁴School of Engineering and Science, University of the West of Scotland, Paisley PA1 2BE, UK

¹⁵INRNE, Bulgarian Academy of Sciences, 1784 Sofia, Bulgaria

Abstract. A fast-timing experiment was performed at the Argonne National Laboratory to measure the lifetimes of the lowest lying states of nuclei belonging to the deformed regions around mass number $A \approx 110$ and $A \approx 150$. These regions were populated via spontaneous fission of ^{252}Cf and the gamma radiation following the decay of excited states in the fission fragments was measured using 51 Gammasphere detectors coupled with 25 LaBr₃:Ce detectors. A brief description of the acquisition system and some preliminary results from the fast-timing analysis of the fission fragment ^{100}Zr are presented. The lifetime value of $\tau = 840(65)$ ps was found for the 2^+ state in ^{100}Zr consistent within one standard deviation of the adopted value with 791^{+26}_{-35} ps. This is associated with a quadrupole deformation parameter of 0.36(2) which is within one standard deviation of the literature value of 0.3556^{+82}_{-57} .

*e-mail: E.Gamba@brighton.ac.uk

1 Introduction

The aim of the experiment was to measure the evolution of the quadrupole deformation in nuclei around mass numbers $A \approx 110$ and $A \approx 150$. The lifetime of the first excited state is an essential ingredient in the calculation of the reduced transition probability $B(E2)$ which gives, in turn, the quadrupole moment which is related to the deformation parameter. Therefore important information about the evolution of the deformation can be obtained from lifetime measurements of these low-lying levels. In order to populate these mass regions a source of ^{252}Cf was used. As shown in Fig. 1 a), the spontaneous fission of this isotope has a higher fission yield for $A \approx 110$ nuclei as compared to ^{240}Pu and $^{234,236}\text{U}$. In Fig. 1 b) the independent yield, taken from [1], for every fission product, is given.

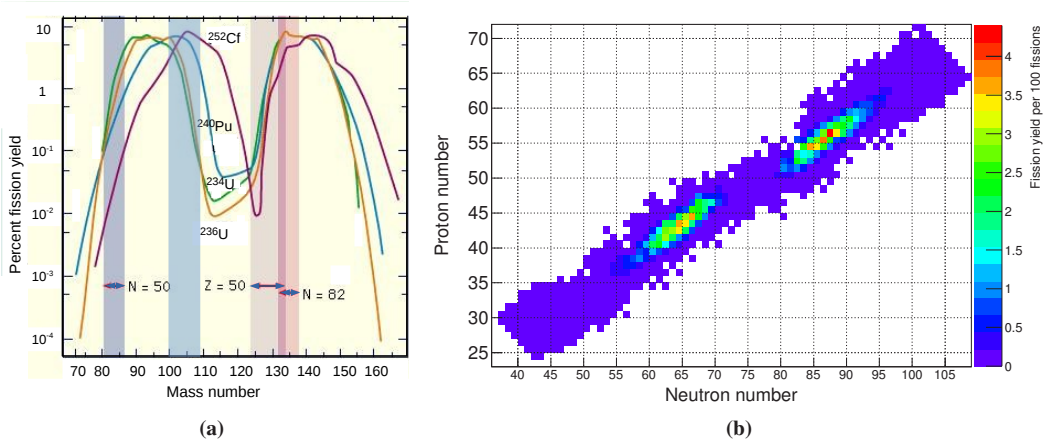


Figure 1. (a) Spontaneous fission yields for ^{252}Cf (purple line), compared to the thermal neutron-induced fission yields for ^{234}U (yellow), ^{236}U (green) and ^{240}Pu (blue), adapted from Ref. [2]. (b) Fission yields for ^{252}Cf source per 100 fission processes. The independent yield value ignores any contributions given by the eventual decay of other nuclei, following the fission process.

The experimental setup combined the superior energy resolution of HPGe Gammasphere detectors with the timing properties of $\text{LaBr}_3:\text{Ce}$ detectors, known to be able to access the sub-nanosecond range of nuclear lifetimes [3, 4]. $\text{LaBr}_3:\text{Ce}$ scintillators have been coupled with the Gammasphere array in the past [5], but this is the first time that the HPGe array was used in coincidence with such a large number of $\text{LaBr}_3:\text{Ce}$ detectors. Fast-timing measurements using $\text{LaBr}_3:\text{Ce}$ scintillator detectors have already been successfully performed, for example at RIKEN [6] and during the EXILL-FATIMA campaign [4]. The experiment was also a benchmark case for implementing a digital acquisition system for the 25 $\text{LaBr}_3:\text{Ce}$ detectors of the UK NuSTAR collaboration [7, 8].

2 The hybrid array and its setup

A hybrid array comprising 51 Gammasphere HPGe detectors and 25 $\text{LaBr}_3:\text{Ce}$ detectors, arranged in a 4π geometry, was used for this experiment. Each $\text{LaBr}_3:\text{Ce}$ detector consisted of a $1.5'' \times 2''$ cylindrical crystal coupled with a R9779 Hamamatsu PMT. Lead shields were used to avoid cross-talk events between neighbouring detectors. A typical $\text{LaBr}_3:\text{Ce}$ rate for one single detector was 2.7 kHz. Each of the two arrays had its own acquisition chain which worked independently. On the $\text{LaBr}_3:\text{Ce}$

side, electronics based on the VME standard was used while the Digital Gammashpere (DGS) acquisition system was used for the HPGe array. The coupling was accomplished via the MyRIAD module [9] which synchronises the clocks from the two DAQ systems. A detailed description of the two DAQs is given in Ref. [10, 11] for the DGS, and in Ref. [12] for the LaBr₃:Ce coupled with DGS. The stand-alone DGS collected 2-fold events for spectroscopic studies, with a coincidence window of 2 μs, and these were stored as an independent data set. A second data set, used for fast-timing purposes, consisted of 2-fold events in the LaBr₃:Ce array in coincidence with at least one gamma ray detected in Gammashpere. The coincidence window between two LaBr₃:Ce detectors was 200 ns, while the window between Gammashpere and the LaBr₃:Ce array was set to 500 ns.

3 Preliminary results

The preliminary data analysis described in this section is intended to explain how a typical lifetime measurement is performed using this setup and, as an example, the procedure used to obtain the lifetime of the 2⁺ state in ¹⁰⁰Zr, is described. The nuclei of interest are identified by applying energy gates on the transitions measured in Gammashpere. The gate conditions usually consist of selecting two transitions of known energy originating either from the nucleus of interest or taking one gamma ray from the nucleus of interest and one gamma ray from its fission partners. The data obtained from these different combinations of gates, can then be added together in order to improve the statistics. This has been done for all the combinations between one transition in the ground state band of ¹⁰⁰Zr and one transition in the ground state band of its fission partner ¹⁴⁸Ce. For both nuclei, only transitions up to 10⁺ → 8⁺ are being considered, and the 4⁺ → 2⁺ and 2⁺ → 0⁺ transitions in ¹⁰⁰Zr are excluded since they will be used later on to obtain the time distribution of the 2⁺ level. This gives a total of 15 pairs of gates. The gamma-ray energy spectra obtained by applying each one of these pairs of gates to the data, have been added together and the sum spectrum is shown in Fig. 2 a). Fig. 2 b) shows the gamma-ray spectrum with no gates applied and is presented for comparison purposes. At this stage of the analysis no background subtraction has been performed.

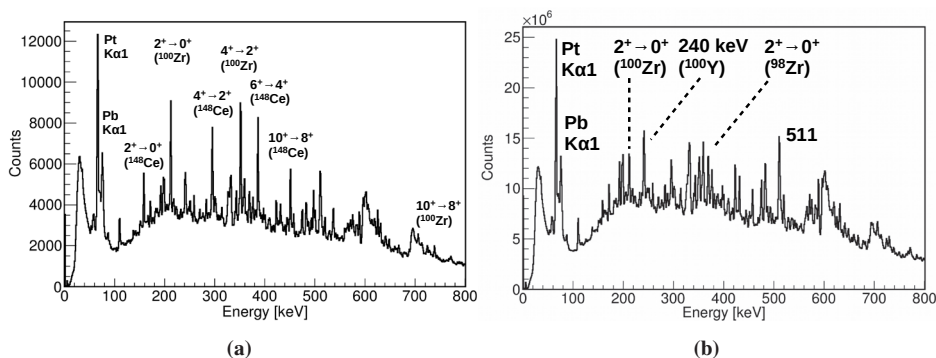


Figure 2. The sum HPGe energy spectrum (a) with 15 different pairs of gates applied. The gamma rays from ¹⁰⁰Zr and ¹⁴⁸Ce are present in this spectrum and (b) with no gates applied.

In Fig. 3 a comparison between the background-subtracted, triple-gated DGS spectrum (blue) and LaBr₃:Ce spectrum (red) is shown. They represent event of the type Ge-Ge-Ge-Ge and Ge-Ge-LaBr-LaBr respectively, where the first two coincident gamma rays are inside any pair of gates in the HPGe

array, as described above. Both the event types have then been gated on the $4^+ \rightarrow 2^+$ transition in ^{100}Zr , at 352 keV. The surroundings of the peak at 212 keV (the $2^+ \rightarrow 0^+$ transition) is relatively clean.

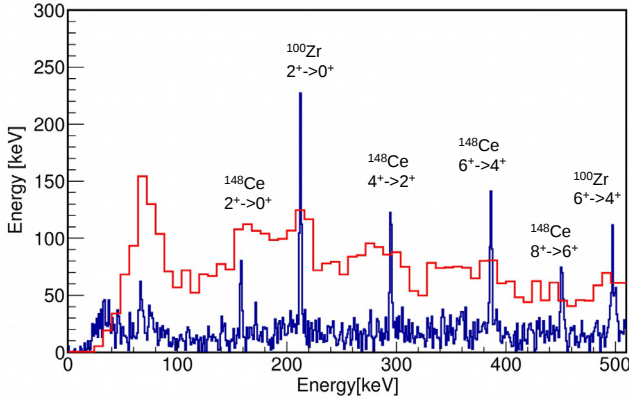


Figure 3. Gamma rays measured in HPGe (blue) and LaBr₃:Ce (red) in coincidence with 15 pairs of gates in the HPGe and the $4^+ \rightarrow 2^+$ transition in ^{100}Zr . The region surrounding the peak at 212 keV ($2^+ \rightarrow 0^+$) is shown to be relatively clean (see text for details).

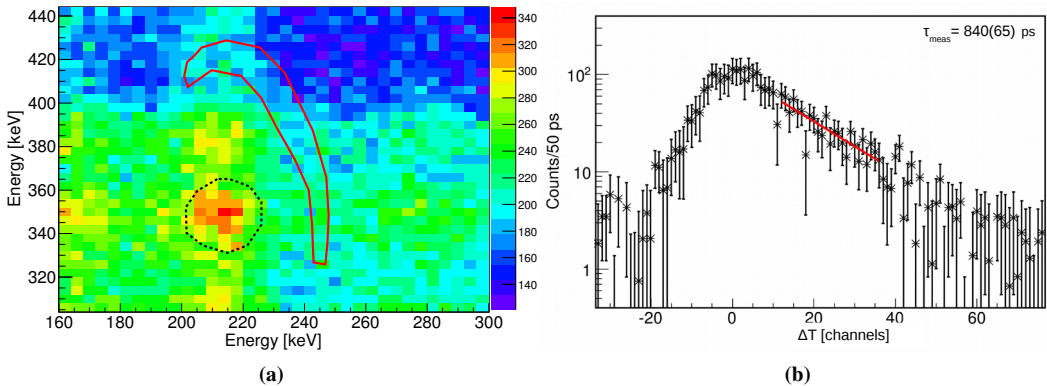


Figure 4. (a) LaBr₃:Ce gamma-gamma energy matrix obtained after gating on 15 pairs of transitions, belonging to the nuclei ^{100}Zr and ^{148}Ce , in the HPGe detector array. The black dotted line encircles the coincidence peak between the $4^+ \rightarrow 2^+$ and $2^+ \rightarrow 0^+$ transitions in ^{100}Zr , while the red solid line gives the background spectrum. (b) LaBr₃:Ce background-subtracted time distribution of the $2^+ \rightarrow 0^+$ transition in ^{100}Zr . The fit has been performed on different regions, far from the prompt peak and the background region, and the average value has been extrapolated.

The time information is extracted using the data from the LaBr₃:Ce detectors. Fig. 4 a) shows the gamma-ray energies measured in the LaBr₃:Ce detectors in coincidence with the 15 pairs of transitions in HPGe detectors. The figure focuses around the region of the $4^+ \rightarrow 2^+$ (352 keV) and $2^+ \rightarrow 0^+$ (212 keV) transitions in ^{100}Zr . The black dotted line in Fig. 4 a) shows the gate on the $4^+ \rightarrow 2^+ \rightarrow 0^+$ gamma-ray cascade, used to obtain the time distribution of the first 2^+ state in ^{100}Zr . This is presented in Fig. 4 b) and it represents the case where the $4^+ \rightarrow 2^+$ and $2^+ \rightarrow 0^+$ transitions in ^{100}Zr were used as start and stop, respectively. The background time distribution was obtained by

gating on the region inside the red solid curve, and normalising with respect to the number of bins. Work is still progressing and it hasn't been decided what is the best background subtraction procedure to be used (if any) and the one presented in this work is just one among different approaches which are currently under analysis, for this test case.

A lifetime value $\tau = 840(65)$ ps was obtained for the 2^+ state by fitting the time spectrum with an exponential decay function in the region far from the prompt peak, as shown in Fig 4 b). This contribution presents the first lifetime measurement obtained from this data set after two gates on the Gammasphere energy information have been applied. It shows a step forward in the analysis with respect to the results presented in [12], where only one gate on the Gammasphere data was employed and a lifetime of $\tau = 827(108)$ ps was obtained using the decay slope fitting method. In Fig. 5 this preliminary result is shown to be within one standard deviation of the recommended value from Ref. [13] of 791^{+26}_{-35} ps. This recommended value doesn't include the most recent measurement of $820(30)$ ps obtained in Ref. [4] by means of the slope method, using 16 LaBr₃:Ce detectors from the same collaboration. The present result is also within one standard deviation of this most recent value.

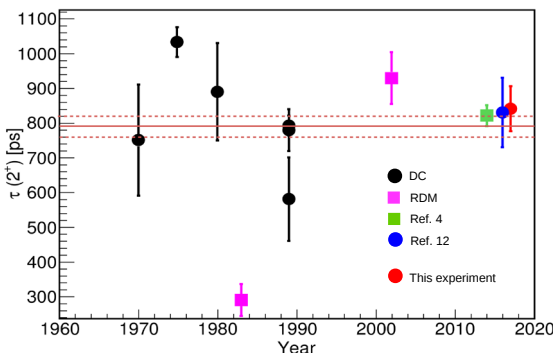


Figure 5. Previous values of the lifetime of the 2^+ state in ^{100}Zr . DC stands for delayed coincidence and RDM stands for recoil distance method. The brown line shows the weighted average of 791^{+26}_{-35} ps of all measurements prior to 2010, from Ref. [13]. The value of $840(65)$ ps from this experiment lies within one standard deviation of this value (red dot). The measurement made in Ref. [4] and Ref. [12] are represented by the green square and the blue dot, respectively.

On the assumption of an axially symmetric shape, the quadrupole deformation parameter β_2 , associated with this lifetime value, was calculated to be $0.36(2)$, which is within one standard deviation of the literature value of 0.3556^{+82}_{-57} [13].

4 Conclusions

To summarize, the experiment is producing reliable results even though the analysis is still a work in progress. For the first time the capability of this setup to produce a valid time distribution after a double gate on the energy information from Gammasphere has been shown, and the results are in good agreement with the values given in the literature. Shorter lifetimes will also be investigated using the *Generalized Centroid Shift Method* (GCD) described in Ref. [14]. This has already been tested for our setup, using the known lifetimes of the 4^+ and 6^+ states in ^{166}Er , populated via the beta-decay of a ^{166}Ho source. The values obtained were $173.1(43)$ ps and $19.8(46)$ ps respectively, both within one standard deviation of the literature values of $170(6)$ ps and $21.6(11)$ ps [15]. More details are presented in Ref. [12] which also shows that, given good statistics and peak to background ratio, it should be possible to measure lifetimes down to 10 ps.

In the next future, neutron-rich zirconium isotopes, further away from stability, will also be investigated. Since mixed multiplicity-three and multiplicity-four events were collected during the experiment, the procedure described in Sec. 3 allows a very selective identification of the nuclei of interest.

This will be used to measure the lifetime of low lying states in the odd-mass zirconium isotopes $^{103,105}\text{Zr}$. At the same time spectroscopic studies can be carried out using the information obtained from HPGe detectors in their stand-alone configuration. In order to get information about the spin of excited states, angular correlations between gamma rays will also be investigated, exploiting the high granularity of this hybrid detector array.

Acknowledgement

UK authors acknowledge the support of the Science and Technology Facilities Council (STFC).
E. Stefanova and O.Yordanov acknowledge the support from BNSF under contract DFNI-E02/6.

References

- [1] T. R. England, B. F. Rider, US reports ENDF-349, LA-UR-34-3106 LANL (1994).
- [2] A.C. Wahl, Symposium on Physics and Chemistry of Fission, IAEA (1965)
- [3] N. Mărginean et al., Eur. Phys. J. A **46**, 329 (2010).
- [4] J.-M. Régis et al., Eur. Phys. J. Conf. **93**, 01013 (2015)
- [5] S. Zhu et al., NIM A **652**, 231 (2011).
- [6] F. Browne et al., Phys. Lett. B **750**, 448 (2015).
- [7] Zs. Podolyák, Rad. Physics. Chem. **95**, 14 (2014)
- [8] S. Lalkovski et al., Acta Phys.Polon. B **47**, 637 (2016).
- [9] T.J. Anderson, MyRIAD user manual, ANL, 2015.
- [10] I-Y.Lee et al., Nucl. Phys A **520**, 641c (1990).
- [11] T.J. Anderson et al., NSS/MIC, 6551368 (2012).
- [12] M. Rudigier et al., Acta Phys.Pol. B **48**, 351 (2017).
- [13] B. Pritychenko et al., Atom. Data and Nuc. Data Tabl. **107**,1(2016).
- [14] J.-M. Régis et al., NIM A **726**, 191 (2013).
- [15] C. M. Baglin, Nuclear Data Sheets **109**, 1(2008)